

# Nonlinear $r$ -Modes in Neutron Stars: Instability of an unstable mode

Philip Gressman, Lap-Ming Lin\*, and Wai-Mo Suen†  
McDonnell Center for the Space Sciences, Department of Physics,  
Washington University, St. Louis, Missouri 63130

N. Stergioulas  
Department of Physics, Aristotle University of Thessaloniki, Thessaloniki 54006, Greece

John L. Friedman  
Department of Physics, University of Wisconsin-Milwaukee, PO Box 413, Milwaukee, Wisconsin 53201  
(Dated: November 4, 2018)

We study the dynamical evolution of a large amplitude  $r$ -mode by numerical simulations.  $R$ -modes in neutron stars are unstable growing modes, driven by gravitational radiation reaction. In these simulations,  $r$ -modes of amplitude unity or above are destroyed by a catastrophic decay: A large amplitude  $r$ -mode gradually leaks energy into other fluid modes, which in turn act nonlinearly with the  $r$ -mode, leading to the onset of the rapid decay. As a result the  $r$ -mode suddenly breaks down into a differentially rotating configuration. The catastrophic decay does not appear to be related to shock waves at the star's surface. The limit it imposes on the  $r$ -mode amplitude is significantly smaller than that suggested by previous fully nonlinear numerical simulations.

PACS numbers: 95.30.Sf, 04.30.Db, 04.40.Dg, 97.60.Jd

The  $r$ -modes of rotating neutron stars are unstable growing modes driven by gravitational radiation reaction [1, 2]. If the  $l = m = 2$   $r$ -mode of a young, rapidly rotating star can grow to an amplitude of order unity, the gravitational radiation it emits would carry away most of the star's angular momentum and rotational kinetic energy; and the radiation might be detectable by the Laser Interferometric Gravitational Wave Observatory (LIGO II) [3] (for recent reviews see [4, 5]). Even if its amplitude were smaller, the  $r$ -mode instability would limit the periods of hot, young neutron stars (and, possibly, of old stars spun up by accretion). A number of mechanisms to damp the mode have been examined, including shear viscosity enhanced by crust-core coupling and by nonstandard cooling [6]; bulk viscosity enhanced by a hyperon-rich core [7]; and energy loss to a magnetic field driven by differential rotation [8]. But none of these definitively eliminates the instability.

The significance of the  $r$ -mode instability depends strongly on its maximum possible amplitude. In two recent Letters, Stergioulas and Font [9] and Lindblom, Tohline, and Vallisneri [10] performed numerical simulations of nonlinear  $r$ -modes, both finding that large-amplitude nonlinear  $r$ -modes can exist for some long period of time. In addition, in [10, 11], Lindblom *et al.* carried out numerical simulations of the growth of the  $r$ -modes driven by the current quadrupole post-Newtonian radiation reaction force in Newtonian hydrodynamics. In order to achieve a significant growth of the  $r$ -mode am-

plitude in a reasonably short computational time, they artificially multiplied the radiation reaction force by a factor of 4500. This decreases the growth time of the  $r$ -mode from about 40 s to 10 ms. The (dimensionless)  $r$ -mode amplitude  $\alpha$  grew to  $\approx 3.3$  before shock waves appeared on the surface of the star and the  $r$ -mode amplitude collapsed. Lindblom *et al.* suggested that the nonlinear saturation amplitude of the  $r$ -modes may be set by dissipation of energy in the production of shock waves. Here, we show that a hydrodynamical effect will restrict the  $r$ -mode amplitude to a value significantly below that reported in [10, 11].

We note that, with the artificially large radiation reaction, the results in [10, 11] assume that no hydrodynamic process takes energy from the  $r$ -mode in a time scale between 10 ms and 40 s (the artificial growth time and the actual physical growth time, respectively). In this paper we investigate the evolution of large amplitude  $r$ -modes in these time scales (10 ms-40 s). We find that (i) a catastrophic decay of the mode, occurring within these time scales, significantly reduces the amplitude to which an  $r$ -mode can grow, and (ii) in a large amplitude  $r$ -mode this catastrophic decay leads to a differentially rotating configuration. (As in Refs. [10, 11], we assume a perfect fluid with no magnetic fields.)

We solve the Newtonian hydrodynamics equations for a non-viscous fluid flow in the presence of gravitational radiation reaction:

$$\frac{\partial \rho}{\partial t} + \nabla \cdot (\rho \vec{v}) = 0, \quad (1)$$

$$\rho \left( \frac{\partial \vec{v}}{\partial t} + \vec{v} \cdot \nabla \vec{v} \right) = -\nabla P - \rho \nabla \Phi + \rho \vec{F}_{\text{GR}}, \quad (2)$$

where  $\rho$  is the density,  $P$  is the pressure,  $\vec{v}$  is the velocity,

\*Corresponding author.

†Also at Department of Physics, The Chinese University of Hong Kong, Hong Kong.

$\vec{F}_{\text{GR}}$  is the radiation reaction force per unit mass, and  $\Phi$  is the Newtonian potential, satisfying

$$\nabla^2 \Phi = 4\pi G\rho. \quad (3)$$

A high resolution shock capturing scheme (Roe solver) is used to solve the hydrodynamic equations. In addition, as in [9], we applied the 3rd order piecewise parabolic method (PPM) [12] for the cell-reconstruction process in order to simulate rapidly rotating stars accurately for a large number of rotational periods.

As  $r$ -modes couple to the gravitational radiation mainly through the current multipoles  $J_{lm}$ , we assume that the contribution to the reaction force  $\vec{F}_{\text{GR}}$  comes solely from the dominant current multipole  $J_{22}$ , an approximation used also in [10, 11]. The resulting expression for  $\vec{F}_{\text{GR}}$  is given by (see [10, 13, 14])

$$F_{\text{GR}}^x - iF_{\text{GR}}^y = -\kappa i(x + iy) \left[ 3v^z J_{22}^{(5)} + z J_{22}^{(6)} \right], \quad (4)$$

$$F_{\text{GR}}^z = -\kappa \text{Im} \left\{ (x + iy)^2 \left[ 3 \frac{v^x + iv^y}{x + iy} J_{22}^{(5)} + J_{22}^{(6)} \right] \right\}, \quad (5)$$

where  $J_{22}^{(n)}$  is the  $n$ th time derivative of  $J_{22}$  and  $\kappa = \kappa_0 \equiv 32\sqrt{\pi}G/(45\sqrt{5}c^7)$ . A technical difficulty in evaluating  $\vec{F}_{\text{GR}}$  is that it depends on high-order time derivatives of  $J_{22}$ . To circumvent this problem, we assume that  $J_{22}^{(n)} = (i\omega)^n J_{22}$ , with the nonlinear  $r$ -mode frequency  $\omega$  defined by  $\omega = -|J_{22}^{(1)}|/|J_{22}|$ , as in [10, 11]. Notice that  $J_{22}^{(1)}$  can be expressed as an integral over the fluid variables and is thus calculated on each time slice [10, 11, 14].

To investigate the dynamical properties of a large amplitude  $r$ -mode numerically, one must first generate initial data. However, analytically we know only the expression of an  $r$ -mode in the linear regime, under the assumption of  $\alpha \ll 1$  and  $\Omega_0 \rightarrow 0$ . In particular, the  $l = m = 2$   $r$ -mode perturbation (at the first order of  $\Omega_0$ ) is given by [15]

$$\delta\vec{v} = \alpha_0 R_0 \Omega_0 \left( \frac{r}{R_0} \right)^2 \vec{Y}_{22}^B e^{i\omega t}, \quad (6)$$

where  $\alpha_0$  is a dimensionless amplitude,  $R_0$  and  $\Omega_0$  are the radius and angular velocity of the unperturbed rotating star model, and  $\vec{Y}_{22}^B$  is the magnetic-type vector spherical harmonic defined by  $\vec{Y}_{lm}^B = [l(l+1)]^{-1/2} \vec{r} \times \nabla Y_{lm}$ . Using Eq. (6) with a large  $\alpha_0$  introduces other modes in the initial data [11]; that is, the resulting configuration is not the same as an  $r$ -mode growing from small amplitude driven by gravitational radiation reaction. In the following, we will show how we obtain a large amplitude  $r$ -mode in our study.

Beyond the linear regime, there is no unique mode decomposition, and hence no unique definition of an  $r$ -mode. In this paper, by a large amplitude  $r$ -mode we mean a configuration resulting from the growth of

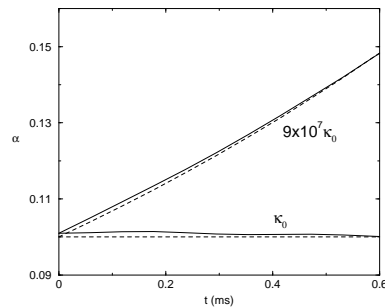


FIG. 1: Evolution of  $\alpha$  in a slowly rotating star with the correct ( $\kappa_0$ ) and artificial ( $9 \times 10^7 \kappa_0$ ) radiation reaction. The solid lines represent the numerical results ( $257^3$  resolution), while the dashed lines are the predictions from linear theory.

an infinitesimal  $r$ -mode due to gravitational radiation reaction. We define the amplitude  $\alpha$  of the nonlinear  $l = m = 2$  mode in terms of its contribution to  $J_{22} = \int \rho r^2 \vec{v} \cdot \vec{Y}_{22}^{B*} d^3x$ :

$$\alpha(t) \equiv \left| \frac{1}{R^3} \int \tilde{\alpha}(x) e^{i\phi(x)} d^3x \right|, \quad (7)$$

$$\tilde{\alpha}(x) e^{i\phi(x)} \equiv \frac{8\pi R^4 \left( \rho r^2 \vec{v} \cdot \vec{Y}_{22}^{B*} \right)}{\Omega(t) \int \rho r^4 d^3x}.$$

Here  $R$  is the radius of the corresponding nonrotating star model and  $\tilde{\alpha}(x)$  is the amplitude density. The phase factor  $\phi(x)$  is defined so that  $\tilde{\alpha}(x)$  is real. The definition of the amplitude is similar to that of [10], except that we normalize  $\alpha(t)$  by the average angular velocity of the star  $\Omega(t)$  instead of a fixed initial  $\Omega_0$ .

In Fig. 1, we show the time evolution of  $\alpha$  for two cases in a slowly rotating star with  $T = 4.42$  ms. In the first case  $\kappa$  is set to the correct Post-Newtonian value  $\kappa_0$  (represented by the solid line labeled “ $\kappa_0$ ”). The evolution begins with a small (linear)  $r$ -mode perturbation given by Eq. (6) with  $\alpha_0 = 0.1$ . The simulation is carried out up to  $t = 0.6$  ms. To compare, we plotted as dashed line the evolution of  $\alpha$  as predicted by the linear theory [15]:  $\alpha = \alpha_0 e^{t/\tau_{\text{GR}}}$ , where the gravitational radiation time scale is given by

$$\frac{1}{\tau_{\text{GR}}} = \frac{G\Omega_0^6}{2c^7} \left( \frac{256}{405} \right)^2 \left( \frac{\kappa}{\kappa_0} \right) \int \rho r^4 d^3x. \quad (8)$$

We note that this formula is correct only to linear order in  $\alpha$  and in  $\Omega$ , and is thus accurate only for (i)  $\alpha \ll 1$  and (ii)  $\Omega_0/\sqrt{G\bar{\rho}} \ll 1$ . While assumption (i) is reasonably good, (ii) is actually not accurate for the model used: rotation period 4.42 ms, corresponding to  $\Omega/\Omega_{\text{max}} \approx 0.25$  ( $\Omega_{\text{max}} \approx 2\sqrt{\pi G\bar{\rho}}/3$  is the Kepler limit, where  $\bar{\rho}$  represents the average density of the star). Nevertheless, the two lines nearly coincide.

With radiation reaction coefficient  $\kappa_0$ , an evolution time  $t \approx 3 \times 10^8$  ms is needed to reach  $\alpha = 1$ . For a  $129^3$  grid-point simulation, this would take  $O(10^{11})$  time

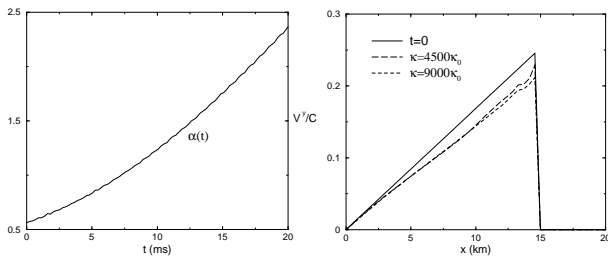


FIG. 2: Left: Growth of the  $r$ -mode amplitude  $\alpha$  during artificial “pumping” with  $\kappa = 4500\kappa_0$ . Right: The velocity profile  $v^y$  along the  $x$  axis at  $t = 0$  and at the point when  $\alpha = 2.0$ .

steps, requiring a clearly impractical  $O(10^8)$  hours on a 128 CPU Origin 2000 (MIPS R12000).

To arrive at a large amplitude  $r$ -mode we use an artificially large  $\kappa$  as in [10, 11]. In Fig. 1, the solid line labeled “ $9 \times 10^7 \kappa_0$ ” represents the evolution of  $\alpha$  with  $\kappa = 9 \times 10^7 \kappa_0$ . For comparison, we also plot the evolution of  $\alpha$  as predicted by the linear theory with this  $\kappa$  as the dashed line. The slight offset between the dashed and solid lines at the initial time is due to the fact that  $\alpha(t = 0)$  as calculated from Eq. (7) equals to  $\alpha_0$  as defined in Eq. (6) only in the limit  $\alpha_0 \ll 1$  and  $\Omega_0 \rightarrow 0$ .

In Fig. 2 (left), we show the growth of an  $r$ -mode (with  $\alpha_0 = 0.5$ ) to a large amplitude with an artificial  $\kappa$  of  $4500\kappa_0$  in our fast rotating star model: The star has a mass of  $M = 1.64M_\odot$  with a polytropic equation of state  $P = k\rho^2$ . The equatorial radius  $R_e = 14.5$  km. The ratio of the polar to equatorial radii is 0.76. The rotation period is  $T = 1.24$  ms. This model is used for the rest of the simulations discussed in this paper. Unless otherwise noted, we use  $129^3$  Cartesian grid points with  $\Delta x = \Delta y = \Delta z = 0.42$  km.

In Fig. 2 (left), the amplitude  $\alpha$  rises from 0.5 to 2.2 in 19 ms. An indicator of the accuracy of the simulation is that the total mass of the system is constant to 0.08% by 20 ms in our  $129^3$  runs. Also, the actual numerical evolution of the total angular momentum  $J = |\int \rho \vec{r} \times \vec{v} d^3x|$  agrees with the theoretical prediction [see Eq. (11) of Ref. [10]] to about 1%.

While the discussion above shows the accuracy of our numerical treatment, one still must ask whether the large amplitude  $r$ -mode obtained with the large artificial pumping is physical or not, in the sense that whether the rapid pumping excites modes that would not be excited with  $\kappa = \kappa_0$ . We compare the large amplitude  $r$ -modes obtained with different pumping rates and conclude that the resulting fluid flow pattern does not depend sensitively on the pump rate (as long as the pump rate is large enough so that the large amplitude  $r$ -mode can be arrived at). In Fig. 2 (right), we show the rotational velocity profile  $v^y$  along the  $x$  axis for  $\kappa = 9000, 4500\kappa_0$  at the point when  $\alpha = 2.0$ , starting with the same initial model. For comparison, we also plot the initial profile in the same figure. We see that the two lines,  $\kappa = 9000, 4500\kappa_0$ , agree with each other to better than 3%, with smaller discrep-

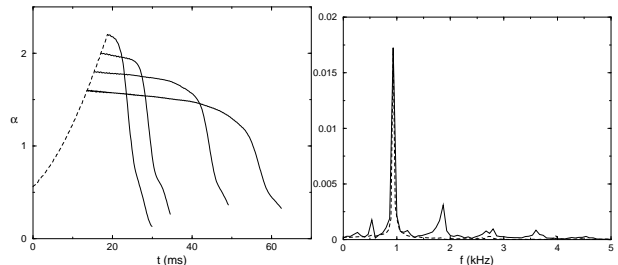


FIG. 3: Left: Evolution of the “pumped up”  $\alpha$  at different values with  $\kappa = \kappa_0$ . Right: Fourier spectra of  $v^z$  along the  $x$  axis (at  $x = 6$  km) at two time slots in the evolution starting out with  $\alpha = 1.6$ . The early (later) time slot is denoted by the dashed (solid) line.

ancy away from the surface. In the rest of this paper, we will take the “pumped up” configurations given in Fig. 2 (left) as the initial state in our investigation of the hydrodynamical behavior of the large amplitude  $r$ -mode. To the extent that different pumping rates are not affecting the initial state we use, the artificial pumping is not affecting the results we report below.

Here we focus on one question: What is the fate of a large-amplitude  $r$ -mode in a rapidly rotating neutron star for a sufficiently long time evolution, modeled as the 1.24 ms polytrope described above. That is, what evolution is implied by Eqs. (1)-(3), with the correct amount of radiation reaction?

In Fig. 3 (left) we show the evolution of  $\alpha$  vs time for various large amplitude  $r$ -modes starting off with  $\alpha = 2.2, 2.0, 1.8, 1.6$ . We see that the mode amplitudes start off slowly decaying, leaking energy to other modes. The decay rate is small, until a certain time. We plot in Fig. 3 (right) the Fourier transform of the velocity component  $v^z$  along the  $x$  axis at a typical point inside the star at two different time slots in the evolution of the  $\alpha = 1.6$  case [the lowest line in Fig. 3 (left)]. The dashed line is the profile at the beginning of the evolution (13 ms-35 ms), we see that there is only one large peak at the  $r$ -mode frequency (0.93 kHz). This is compared to the solid line representing the spectrum at a later time slot (35 ms - 50 ms). We see that various smaller peaks appear in the spectrum, especially the one at twice the  $r$ -mode frequency (1.86 kHz). Spectra at different points inside the star give similar structure, with those in the core region showing more peaks at different frequencies.

The most interesting feature of Fig. 3 (left) is that after some slow leaking of energy into other fluid modes, the  $r$ -mode amplitude drops catastrophically to a value much smaller than 1. This abrupt drop occurs through nonlinear couplings with other fluid modes: In the slow leaking phase, these other fluid modes are growing linearly until a certain unstable point. The time it takes to reach the unstable point depends sensitively on the  $r$ -mode amplitude. It shortens from approximately 45 ms to 8 ms when the initial value of  $\alpha$  changes from 1.6 to 2.2.

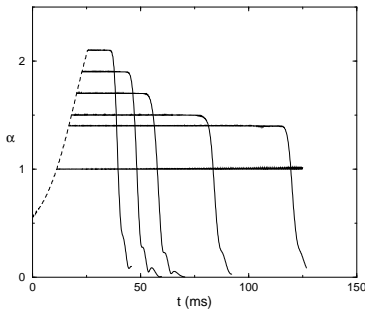


FIG. 4: Evolution of  $\alpha$  ( $65^3$  resolution) with artificial pumping of  $\kappa = 4500\kappa_0$  whenever  $\alpha$  drops below its initial value.

To further investigate this catastrophic decay we perform a set of numerical experiments in which we pump energy into the  $r$ -mode by turning on the artificial radiation reaction force with coefficient  $\kappa = 4500\kappa_0$  whenever its amplitude drops down below its initial value. The resulting evolution of  $\alpha$  vs time is given in Fig. 4. The evolution tracks of  $\alpha$  starting off with values  $\alpha = 2.1, 1.9, 1.7, 1.5, 1.4, 1.0$  are given. With the large artificial pumping  $\alpha$  remains constant despite energy leaking to other modes. In all cases (except  $\alpha = 1.0$  where the simulation is not evolved long enough), however, the hydrodynamical nonlinear interaction eventually overwhelms the artificial pumping, and the  $r$ -mode amplitude falls catastrophically.

In Fig. 5 we compare the distribution of the amplitude density  $\tilde{\alpha}(x)$  as defined in Eq. (7) on the equatorial plane before (left) and after (right) the breakdown respectively for the case where the initial  $\alpha$  is 2.0 (the  $\alpha = 2.0$  line in Fig. 3). In the figure, the brighter region represents higher amplitude density. During the catastrophic decay, the  $r$ -mode pattern changes rapidly from a 4-fold “regular” shape (left) to a whirlpool-like spiral (right). We also see in our simulations that strong differential rotation is developed during the breakdown, a potentially important fact regarding whether subsequent re-growth of the  $r$ -mode is possible or not [16].

In Fig. 6 we plot the rotational velocity profile  $v^y$  along

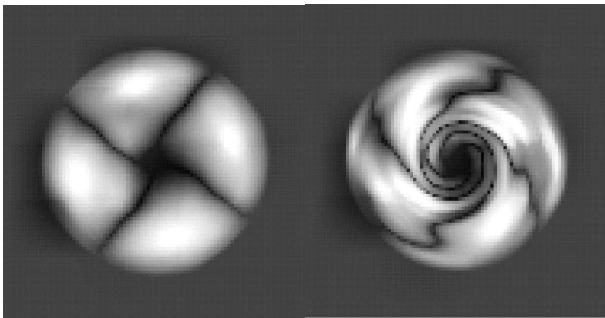


FIG. 5: The amplitude density  $\tilde{\alpha}(x)$  on the equatorial plane before (left) and after (right) the breakdown for the case where the initial “pumped up”  $\alpha$  is 2.0 in Fig. 3.

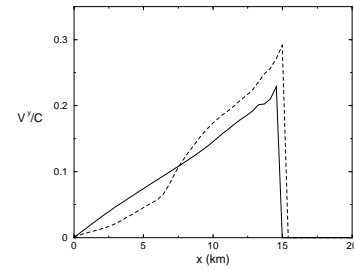


FIG. 6: The rotational velocity profile  $v^y$  along the  $x$  axis for the case where the initial “pumped up”  $\alpha$  is 2.0. The solid line is the initial profile at  $\alpha = 2.0$ , while the dashed line is the profile after the breakdown.

the  $x$  axis for the case where the initial  $\alpha$  is 2.0. The solid line is the initial profile, while the dashed line is the profile after the decay. To further quantify the amount of differential rotation, we define the kinetic energy associated to differential rotation by  $I = \frac{1}{2} \int \rho (v_\phi - \bar{v}_\phi)^2 d^3x$ , where  $\bar{v}_\phi = \bar{\Omega} \sqrt{x^2 + y^2}$  with  $\bar{\Omega}$  being the average angular velocity of the star. We plot the evolution of  $\alpha$  and  $I$  together in Fig. 7 (left). It is seen that the amount of differential rotation ( $I$ ) rises rapidly during the breakdown of  $\alpha$ . We also see in our simulations that the star has a relatively large amplitude pulsation during the breakdown. Fig. 7 (right) shows the quadrupole-moment component  $Q_{xy}$  against time for the same case as in Fig. 7 (left). We see that  $Q_{xy}$  is basically zero until the breakdown and it then oscillates rapidly afterward. However, based on an order-of-magnitude estimation, the gravitational radiation amplitude due to the changing quadrupole moment is only about 1% of that due to the  $r$ -mode.

In contrast to the study of Refs. [10, 11], we do not see evidence that this catastrophic decay is due to the generation of shock waves on the surface of the star.

We found in this paper that a large amplitude  $r$ -mode will lose energy to other fluid modes whose growth in turn trigger a catastrophic decay of the  $r$ -mode. For an  $r$ -mode with an amplitude  $\alpha$  of order one, the onset of catastrophic decay requires a time much shorter than the growth time of the  $r$ -mode due to radiation reaction; and

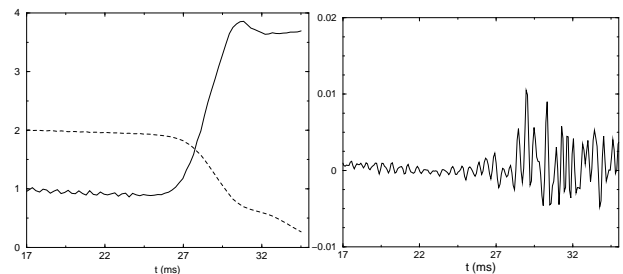


FIG. 7: Left: Evolution of  $\alpha$  (dashed) and  $I$  (solid) for the case where the initial “pumped up”  $\alpha$  is 2.0. Note that  $I$  has been rescaled for comparison. Right: Evolution of  $Q_{xy}$  (in  $G = c = M_\odot = 1$  units) for the same case.

the decay thus limits the  $r$ -mode amplitude to a value less than that found by [10, 11]. Further work is in progress to determine the nature of this catastrophic decay, whether it is related to any known hydrodynamical instability of nonlinear flow, and how large an  $r$ -mode amplitude can be with this effect taken into account.

*Note added.* Towards the end of the preparation of this paper we learned the results of Arras *et al.* [17]. We note the following differences between the hydrodynamical phenomenon studied in this paper and that studied by them: The work of Arras *et al.* points to a slow leakage of the  $r$ -mode energy into some short wavelength oscillation modes, leading to an equilibrium distribution of mode amplitudes. This in turn, through viscosity dissipation, limits the  $r$ -mode amplitude to a small value. In this paper we find a sudden and complete breakdown of the  $r$ -mode that operates independent of viscosity. Further numerical investigation will be carried out to investigate the interactions of  $r$ -modes with other oscillation modes. Such investigation is beyond the resolution power

of our present simulations. Note that, if the conclusions of [17] are correct, there may be no astrophysical situation in which  $r$ -modes grow to amplitudes large enough to exhibit the sudden decay seen in our simulations.

We thank N. Andersson, G. Comer, E. Evans, S. Iyer, L. Lindblom, M. Miller, Y. Mino, B. Owen and C. Will for useful discussions. The simulations in this paper made use of the following code components: Newton\_evolve (Newtonian gravity and evolution) by P. Gressman, PPM (PPM reconstruction) by T. Font, Newton\_anal (modules for various Newtonian analyses) by L.-M. Lin, and the Cactus computational toolkit by T. Goodale *et al.* The research is supported by NSF Phy 00-71044, 00-96522, 99-79985 (KDI Astrophysics Simulation Collaboratory Project), NRAC MCS93S025, the EU Programme “Improving the Human Research Potential and the Socio-Economic Knowledge Base” (Research Training Network Contract HPRN-CT-2000-00137), KBN-5P03D01721, and support from the NASA AMES NAS.

- 
- [1] N. Andersson, *Astrophys. J.* **502**, 708 (1998).  
 [2] J. L. Friedman and S. M. Morsink, *Astrophys. J.* **502**, 714 (1998).  
 [3] B. J. Owen *et al.*, *Phys. Rev. D* **58**, 084020 (1998).  
 [4] N. Andersson and K. D. Kokkotas, *Int. J. Mod. Phys. D* **10**, 381 (2001).  
 [5] J. L. Friedman and K. H. Lockitch, gr-qc/0102114.  
 [6] N. Andersson, D. I. Jones, K. D. Kokkotas, and N. Stergioulas, *Astrophys. J.* **534**, L75 (2000); M. Rieutord, astro-ph/0003171; L. Lindblom, B. J. Owen and G. Ushomirsky, *Phys. Rev. D* **62**, 084030 (2000); Y. Levin and G. Ushomirsky, *Mon. Not. R. Astron. Soc.* **324**, 917 (2001); Y. Wu, C. D. Matzner, and P. Arras, *Astrophys. J.* **549**, 1011 (2001); G. Mendell, *Phys. Rev. D* **64**, 044009 (2001).  
 [7] P. B. Jones, *Phys. Rev. Lett.* **86**, 1384 (2001); P. B. Jones, *Phys. Rev. D* **64**, 084003 (2001); L. Lindblom and B. J. Owen, *Phys. Rev. D* **65**, 063006 (2002); P. Haensel, K. P. Levenfish, and D. G. Yakovlev, astro-ph/0110575.  
 [8] H. C. Spruit, *Astron. Astrophys.* **341**, L1 (1999); L. Rezzolla, F. K. Lamb, and S. L. Shapiro, *Astrophys. J.* **531**, L139 (2000); L. Rezzolla, F. K. Lamb, D. Markovic, and S. L. Shapiro, *Phys. Rev. D* **64**, 104013 and 104014 (2001).  
 [9] N. Stergioulas and J. A. Font, *Phys. Rev. Lett.* **86**, 1148 (2001).  
 [10] L. Lindblom, J. E. Tohline, and M. Vallisneri, *Phys. Rev. Lett.* **86**, 1152 (2001).  
 [11] L. Lindblom, J. E. Tohline, and M. Vallisneri, *Phys. Rev. D* **65**, 084039 (2002).  
 [12] P. Collela and P. R. Woodward, *J. Comput. Phys.* **54**, 174 (1984).  
 [13] L. Blanchet, *Phys. Rev. D* **55**, 714 (1997).  
 [14] L. Rezzolla *et al.*, *Astrophys. J.* **525**, 935 (1999).  
 [15] L. Lindblom, B. J. Owen, and S. M. Morsink, *Phys. Rev. Lett.* **80**, 4843 (1998).  
 [16] S. Karino, S. Yoshida, and Y. Eriguchi, *Phys. Rev. D* **64**, 024003 (2001).  
 [17] P. Arras *et al.*, astro-ph/0202345.